Delamination of carbon-fiber strengthening layer from concrete beam during deformation (infrared thermography)

I. N. Shardakov, A. P. Shestakov
Institute of Continuous Media Mechanics of the Ural Branch of Russian Academy of Science (ICMM UB RAS), Korolev str., 1, Perm, 614013, Russia.
shardakov@icmm.ru, shap@icmm.ru

A.A. Bykov
Perm National Research Polytechnic University, Komsomolsky ave., 29, Perm, 614990, Russia
violentharpy@ya.ru

ABSTRACT. Technology of strengthening reinforced concrete structures with composite materials has found wide application. The effectiveness of strengthening of concrete structures with externally bonded reinforcement is supported by a great deal of experimental evidence. However, the problem of serviceability of such structures has not been adequately explored. The present work describes the results of experimental studies on the load-carrying capacity of concrete beams strengthened with carbon fiber reinforced plastic (CFRP). Special emphasis is placed on studying the debonding of the strengthening layer from the concrete surface and analyzing its influence on the load-carrying capacity of beams. Infrared thermography is used to detect the first signs of debonding and to assess the debond growth rate.

KEYWORDS. Carbon fiber reinforced plastic; Reinforced concrete beams; Strengthening; Intermediate crack debonding; Infrared thermography; Quality control; Non-destructive testing methods.

Citation: Shardakov, I. N., Bykov, A.A., Shestakov, A. P., Delamination of carbon-fiber strengthening layer from concrete beam during deformation (infrared thermography), Frattura ed Integrità Strutturale, 38 (2016) 331-338.

Received: 02.06.2016
Accepted: 30.08.2016
Published: 01.10.2016

INTRODUCTION

At present, the technology of strengthening reinforced concrete structures with composite materials is extensively used in the constructional industry. There are many studies supporting the efficiency of strengthening of concrete structures with externally bonded reinforcement, but the evaluation of serviceability of such structures is still the problem to be solved.

There are several possible options of failure of composite reinforced concrete beams [1]: rupture of fiber-reinforced plastic, crushing of compressive concrete, shear failure, concrete cover separation, plate and interfacial debonding, and intermediate crack induced interfacial debonding. In designing structures reinforced with composite materials, the liming state of such structures is considered to be the state of structure deformation, at which the debonding of the composite material from the concrete surface occurs. According to Russian (SP 164.1325800.2014, [2]) and American (ACI 440.2R-

08, [3]) regulations, this approach is applied to bending elements reinforced by a strengthening sheet with anchorage and without it.

In works [4-6], a series of tests have been performed to study the deformation behavior of a beam initially subjected to loading up to crack generation and then strengthened with CFRP. Besides, the dependence of the strength and stiffness of such beams on preliminary loading was shown. However in the structural practice the reinforcement of beams is usually performed directly during loading and followed by grouting cracks before gluing CFRP sheet. The question of how such a restoring procedure affects the strength properties of beams has not received enough attention yet. The influence of the degree of debonding on the carrying capacity of beams deserves further studies as well.

This work studies the debonding of CFRP sheet from the surface of reinforced concrete beams subjected to bending loading. During the experiment carried out in the Laboratory at Perm National Research Polytechnic University, we have investigated the strain behavior of beams strengthened until loading and beams strengthened during loading after the appearance of first cracks and their grouting.

Infrared thermography techniques [7, 8] were applied to identify the first signs of debonding. Heat transfer processes develop differently in a multi-layer systems with and without air gaps. The analysis of surface temperature of the beam at its heating and cooling yielded information about the existence and distribution of debonding on the beam surface.

PROGRAM AND METHODS OF TESTING

In our experiments we used concrete beams made of concrete B20 (Group B1) and concrete B35 (Group B2). Totally 22 sample-beams were prepared and tested. The schematic representation of a sample strengthened with steel reinforcement rods and a composite layer is shown in Fig. 1. The choice of such reinforcement was mainly caused by the condition of equal strength for beam elements in bending. Each group of beams (B1 and B2) was divided into 3 series with 3–5 samples in each of them: series A – reference samples (ordinary concrete beams with steel reinforcement); series B – preliminary strengthened beams, i.e beams strengthened by the CFRP before load application; series C – beams strengthened at a certain stage of loading after the appearance of first visible cracks and their grouting. During the strengthening procedure CFRP sheet SikaWrap-230 40 mm width and 0.13 mm thickness was glued to the beam bottom surface using epoxy resin Sikadur-330. Carbon fiber sheet was also fixed with transverse wrapping anchorage by CFRP straps in two support sections of the beam. For the beams of cerise C strengthening procedure additionally included widening and grouting of cracks with a repair compound and crack injection with a low-viscosity epoxy resin before gluing of CFRP. Strain gauges were installed on steel reinforcement rods, the carbon-fiber sheet and the surface of all beams to control deformations along the beam axes.

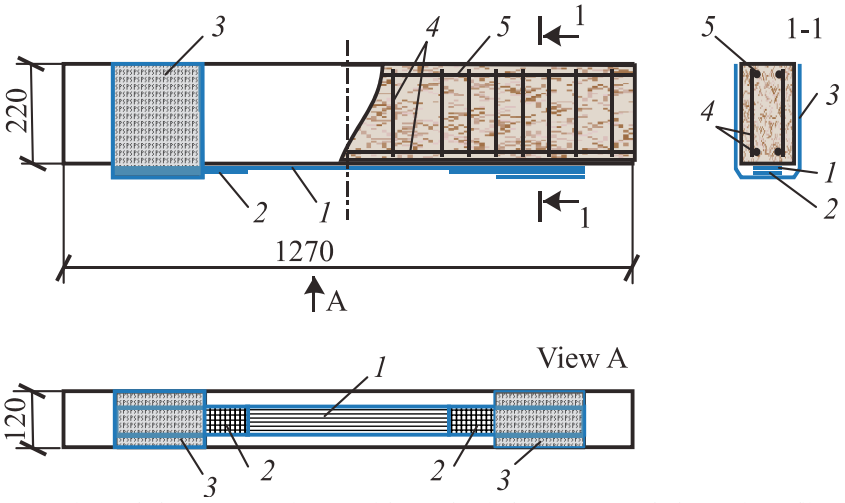

Figure 1: Schematic representation of the concrete beam with steel reinforcement and the carbon fiber strengthening layer: 1 – carbon fiber sheet, 2 – carbon fiber strip, 3 – carbon fiber wrapping anchorage, 4, 5 – steel reinforcement with a diameter of 6 mm and 12 mm, respectively.

The tests were performed on a specially designed four-point bending test set-up (Fig. 2a). The loading of the beams was performed by a successive increasing quasistatic load with a step of 2 kN representing 4–6% of the fracture load. At each

step a 5–10-minute pause was made to record temperature on the stretched surface of the beam. Simultaneously, crack patterns and widths were obtained. To excite heat transfer processes, the beam was subjected to external heat pulse (magnitude of 926 W and duration of 10 sec) and then cooled. Temperature recorded along the whole surface of the CFRP layer using infrared imager FLIR T620 ([9-11]). Shots were taken "through the mirror", which ensured the safety of people and equipment at loads close to the destruction of the beam (Fig. 2b).

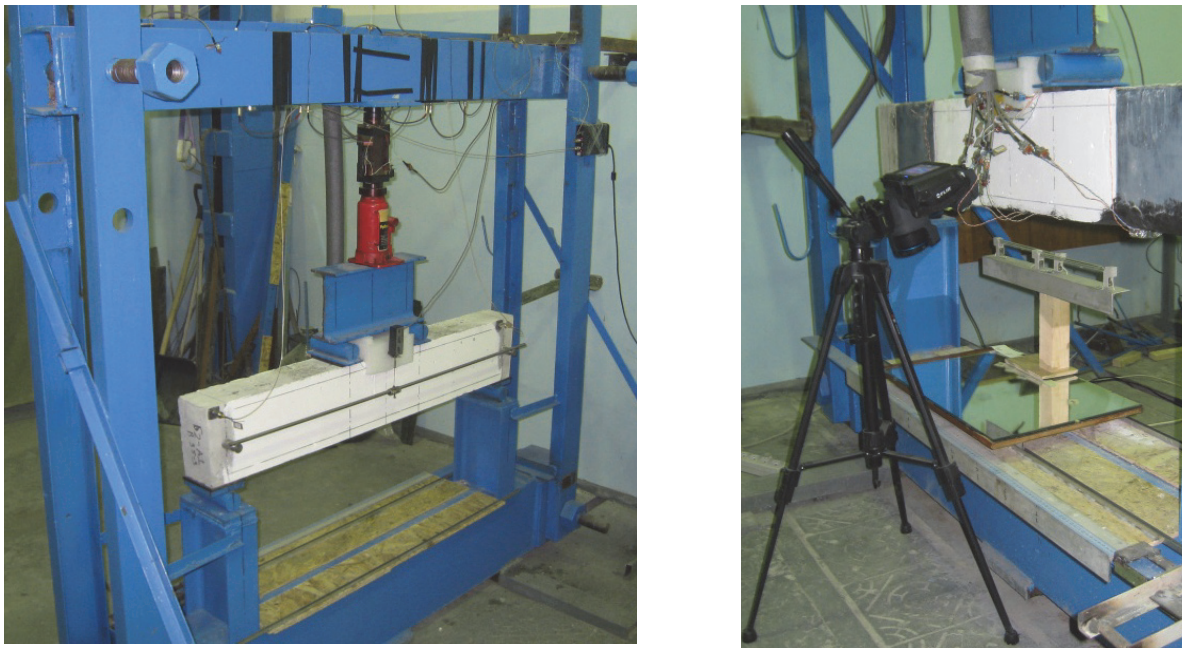

(a) (b)

Figure 2: Load testing machine (a) and infrared shooting arrangement (b).

The details of experimental techniques were determined based on the analysis of the results of numerical solution of nonstationary heat conduction problem in a system of "carbon sheet - epoxy - concrete - delamination - concrete". Difference in surface temperature of the multi-layered system with and without debondings at corresponding instants of time at heating and cooling is called here a temperature response to the presence of delamination. Numerical simulations enabled us to assess the conditions at which the temperature response will be the most. It appears that on heating of the beam by the heat source of 926 W for 10 seconds, the temperature response should be measured at the stage of its cooling, namely 8 seconds after its start (i.e. 18 seconds after the beginning of observation) [12].

Thermography images of the composite surface were obtained at each loading step. The initial thermograms for each j-th step (Fig.3a) is a two-dimensional array of differential temperature values $T_j(x, y)$ determined at 19th and 0th seconds at points with coordinates (x, y). The index $j \in \overline{0, N}$ specifies the number of loading step; loading is absent at $j = 0$. The obtained initial thermograms were processed using an algorithm specifically designed using Matlab programs.

In the first step of the algorithm, we calculate the normalized thermograms

$$TN_j(x, y) = T_j(x, y) T_0(x^*, y^*) / T_j(x^*, y^*)$$

where $T_j(x, y)$ is the initial temperature difference at the j-th loading step at the point (x, y), $T_0(x^*, y^*)$ and $T_j(x^*, y^*)$ are the initial temperature differences at the 0-th and j-th loading steps at the point x^*, y^* where no debonding is known to be present. Normalized thermograms for successive loading steps are given in Fig.3b.

Next the temperature contrast $C_j(x, y)$ (Figure 3c) is determined:

$$C_j(x,y)=\left[TN_j(x,y)-T_0(x,y)\right]/T_0(x,y)\cdot 100\%$$

In order to make a decision on the existence of bebonding at the point with the coordinates (x,y), we calculate a threshold value for the temperature contrast C^*. For making it estimate, we determine, at each loading step, the average value $\overline{C}_j$ and the standard deviation σ_j in those areas of the thermograms, where debonding is known to be absent. The threshold value is calculated by the formula $C^*=\overline{C_j}+3\sigma_j$. The areas of the CRFP layer surface, where the temperature contrast exceeds the threshold value, are identified as the areas with debonding and the remaining ones as the areas free of defect. In the binary defect map shown in Fig.3d, the defect-free areas are shown in white color and the areas of debonding in black color.

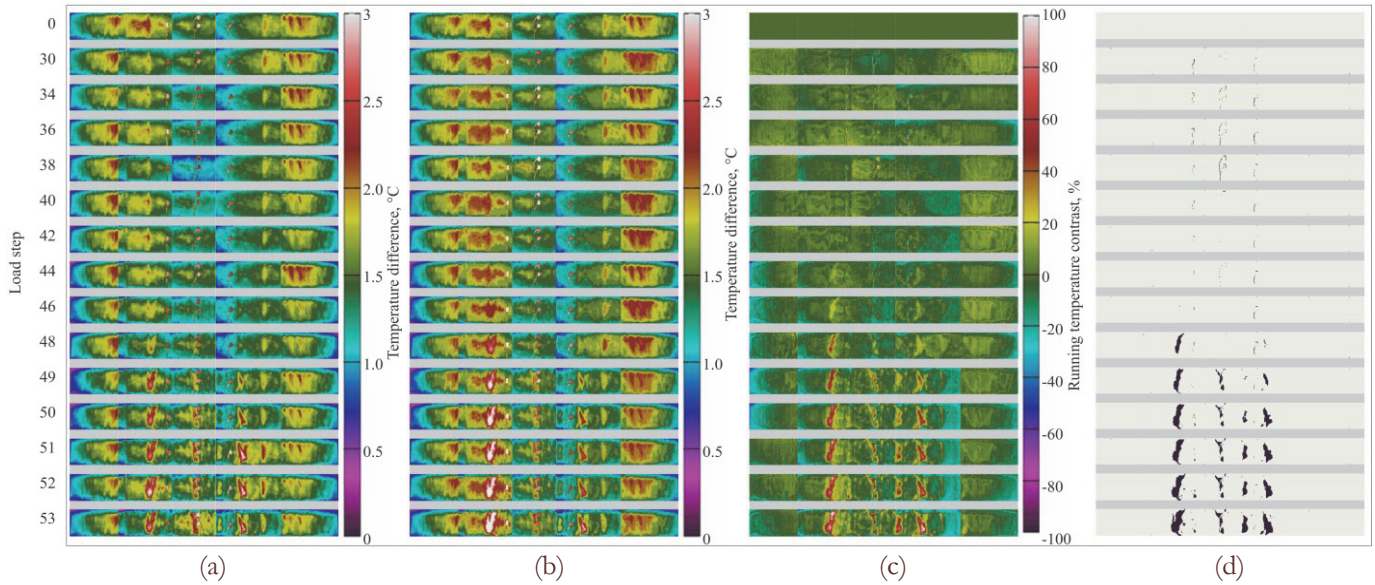

Figure 3: Thermal infrared images obtained using the developed algorithm: (a) initial thermogram; (b) normalized thermogram; (c) temperature contrast map; (d) binary card of defects.

RESULTS AND DISCUSSIONS

The summary data of the static test results for the beams of the series A and B are shown in Tab. 1, the series C – in Tab. 2, where M_{crc} is the bending moment corresponding to the onset of cracking, a_{crc} is the maximum crack opening width, f_{ult} is the elastic deflection, M_{ult} is the maximum bending moment, f_{ult} is the maximum deflection, $\varepsilon_{f,ult}$ is the strain of the carbon-fiber sheet at rupture. Before tests the class of concrete was specified for each beam sample. For the marking of samples were used the following notation: B1 or B2 – groups of concrete, "a", "b", "c" – series, i – sample number.

During the tests we observed two forms of delamination. For the beams, whose surface had been cleaned with a wire brush before sticking CFRP, the delamination occurred according to the adhesive scenario. For the beams, refined with an abrasive tool to a depth of 2-3 mm, the delamination occurred according to the cohesive scenario. For the non-strengthened beams (series A) the destruction state was determined by the rupture of metal reinforcement rods and crushing of the concrete in the compressed zone, for the strengthened ones (series B and C) – by the rupture of CFRP layer, in a number of cases accompanied by the rupture of metal reinforcement.

Fig. 4 shows the dependence of the maximum beam deflection on the bending moment obtained for three series of beams. The comparison of the graphs obtained in the series A and B clearly demonstrates an increase in the bearing capacity of the beams strengthened before loading. The maximum bending moment, which such beams can stand, has happened to be by 37–39% higher than the reference samples. The graphs reflect the appearance of the first cracks in the concrete: it corresponds to a sharp change in the slope angle of the curves.

Specimen	Concrete class	M_{cr}, kNm	Rebound deflection, mm	M_{ult}, kNm	f_{ult}, mm	$a_{crc,max}$, mm	$\varepsilon_{f,ult}$, με	Debonding type	Specimen failure behavior
Bla-1	B25	3.81	0.183	6.13	9.50	2.7	-	-	RR*
Bla-2	B25	3.91	-	7.45	19.84	2.0	-	-	RR+CCC
Bla-3	B25	4.27		6.92	21.43	2.0	-	-	RR*+CCC
Mean value		4.00	0.183	6.83	-	2.2	-	-	-
B1b-1	B25	4.28	-	10.05	14.29	1.1	12170	mixture	FRPR*
Blb-2	B25	5.07	-	10.42	11.16	0.5	11170	mixture	FRPR*
Blb-3	B20	4.33	0.206	10.25	8.30	1.0	13370	cohesion	FRPR
Blb-4	B30	5.40	0.257	10.10	8.08	0.9	12180	cohesion.	FRPR
Blb-5	B20	4.32	0.218	11.07	9.78	1.1	15040	cohesion.	FRPR
Mean (adhesive)	-	4.68	-	10.24	12.72	0.9	11670		-
Mean (cohesive)	-		0.227	10.47	8.72		13530		-
B2a-1	B35	4.74	-	6.98	10.60	1.5	-		RR*
B2a-2	B35	5.15	-	6.98	15.75	7.0	-		RR+CCC
B2a-3	B40	4.98	0.221	7.39	19.73	3.0	-		RR*+CCC
Mean value		4.96	0.221	7.12	-	2.2	-		-
B2b-1	B35	6.14	-	10.03	10.37	0.8	12180	mixture.	FRPR*
B2b-2	B40	5.79	-	10.19	12.52	1.6	10860	adhesion	FRPR*
B2b-3	B40	5.49	0.260	10.56	8.92	1.1	13790	cohesion.	FRPR
B2b-4	B40	5.09	0.213	11.46	9.31	1.0	14280	cohesion.	FRPR
B2b-5	B40	5.43	0.252	10.27	8.06	1.3	12190	cohesion.	FRPR
Mean (adhesive)	-	5.59	-	10.11	11.44	1.1	11520	-	-
Mean (cohesive)	-		0.242	10.76	8.76		13420	-	-

Notes: RR reinforcement rupture, CCC - crushing of compressive concrete, RR* - reinforcement rupture sectional weakened spot welding, FRPR - midspan FRP rupture, FRPR* - FRP rupture sectional strap anchorage, mix. - mixed debonding, coh. - cohesive debonding, adh. - adhesive debonding

Table 1: The results of static test of beams of series A and B.

Specimen	Concrete class	Loading before the appearance of the first cracks: M_{cr}, kNm	Rebound deflection, mm	Maximum bending moment, kNm	$a_{crc,max}$, mm	Bending moment during reinforcement, kNm	Loading after the appearance of the first cracks and their grouting: M_{cr}, kNm	M_{ult}, mm	f_{ult}, mm	$a_{crc,max}$, mm	$\varepsilon_{f,ult}$, με	Debonding type	Specimen failure behavior
Blc-1	B20	3.32	0.142	5.15	1.0	4.30	6.79	10.39	10.80	1.4	11680	cohes.	FRPR
Blc-2	B20	3.60	0.164	5.23	1.5	4.81	7.19	8.75	9.19	1.5	10190	cohes.	FRPR
Blc-3	B30	3.86	0.186	5.20	1.0	4.59	6.59	10.19	11.07	1.3	12760	cohes.	FRPR
Mean value	-	3.60	-	5.19	1.2	4.57	6.86	10.29	-	1.4	11540	-	-
B2c-1	B40	4.30	0.179	5.49	1.0	4.56	6.88	1137	10.29	1.1	14180	cohes.	FRPR
B2c-2	B40	4.92	0.214	5.64	0.9	4.79	7.02	9.03	9.75	1	8655	cohes.	RR*+ FRPR
B2c-3	B40	5.19	0.202	5.52	1.0	4.58	7.69	10.62	10.72	1.3	12430	cohes.	FRPR
Mean value	-	4.80	-	5.55	1.0	4.64	7.19	11.00	-	1.1	13305	-	-

Table 2: The results of static tests of beams of series C.

The evolution of deformation in the beams reinforced under the load is of particular interest. At the initial stage of loading such a beam behaves in the same way as a non- strengthened one (Fig. 4, solid thick lines). The

appearance of the first cracks in the concrete causes a sharp increase in deformation. The subsequent grouting of cracks in the beam under the load leads to the restoration of its rigidity. At this stage, the deformation curve has the "step", on which the slope of the curve is almost restored to its initial value. With a further increase in the bending moment beam displays the same behavior pattern, as the preliminarily strengthened one. The beams strengthened under the load showed an increase in their carrying capacity by 38–49% compared to the non- strengthened samples, and the appearance of the second generation cracks started when the bending moment increased by 45–71%.

In the graphs the loading intervals are marked (circled zones), corresponding to the beginning of cohesive delamination of CFRP. In the beams strengthened under loading delamination begins when the bending moment is on average 75% of the maximum value. Thus, our tests show that the loss of the bearing capacity of the beam cannot be correlated with the beginning of delamination of CFRP layer. As shown in the graphs of Fig. 4, from the beginning of delamination the beam continues to perceive the load and reduction of rigidity does not take place. This means that from the appearance of the first cracks to the total loss of the bearing capacity the beam has some strength reserve which is about 25% of the ultimate load.

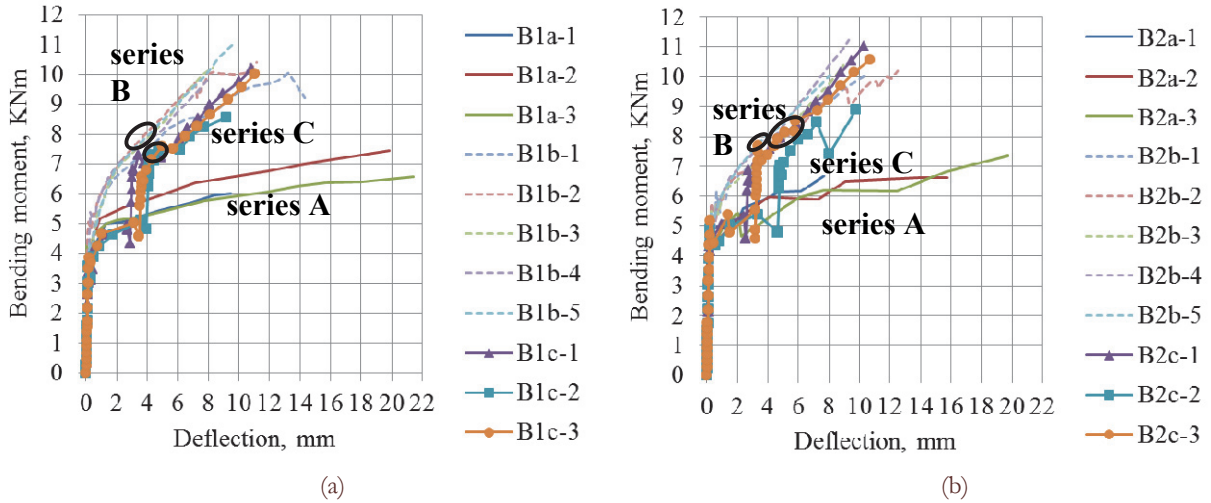

Figure 4: Bending moment–Deflection relationships for series A, B and C: Group B1 (a), Group B2 (b).

The algorithm of thermogram transformation allows one to estimate the relative area of delamination, accumulated in the beams at each loading step. The data presented in Tab. 3 show that the relative area of delamination in the beams reinforced under loading is on average 2.1–2.3 times greater than in the preliminary strengthened ones.

The comparison of the experimental strain values, corresponding to the onset of cohesive delamination of CFRP, with the data theoretically obtained from 5 different methods used in practice, demonstrates a low reliability of these calculation methods (Fig. 5). For instance, the values calculated by the regulatory method used in Russia exceeds the experimentally registered by 15–75% for different classes of concrete.

Conclusion

1. It is shown that for the bearing capacity of CFRP beams destroyed due to the rupture of CFRP does not depend on the point when the strengthening is performed. The beams strengthened before loading and under the load after the appearance of first cracks and their grouting demonstrate the bearing capacity that is higher by 37–39% and 38-49%, respectively, than the ordinary CR beams. Grouting of cracks in the beams under loading allows one to increase the limiting value of the bending moment by 45–71% compared to the unstrengthened beams.

2. It is established that the process of CFRP delamination in the beams strengthened under loading begins at strain which is 4-65% lower and the relative area of delamination is 2.1-2.3 times higher compared to the beams strengthened before loading.

3. The onset of delamination of CFRP sheet corresponds to the bending moment, which is 75% of the limit value. Thus, the presence of delamination does not determine the limiting state of CFRP beams with anchorage of CFRP tape on the bearings. Therefore, it is possible to use the breaking strain of the composite as a limiting value of deformations in the limit state design. The existence of cohesive delamination does not reduce the stiffness of the reinforced structure.

Specimen	Binary card of defects	The relative area of the delamination, % particular value	Average value	CFRP strain, με
B1b-3		7.8		10300
B1b-4		12.99	9.71	10660
B1b-5		8.34		10140
B1c-1		19.77		10280
B1c-2		22.59	22.93	8020
B1c-3		26.43		10240
B2b-3		11.78		10810
B2b-4		20.18	14.90	10200
B2b-5		12.73		10070
B2c-1		17.86		8970
B2c-2		33.08	32.41	7220
B2c-3		46.29		10450

Table 3: The results of static tests of beams of series C.

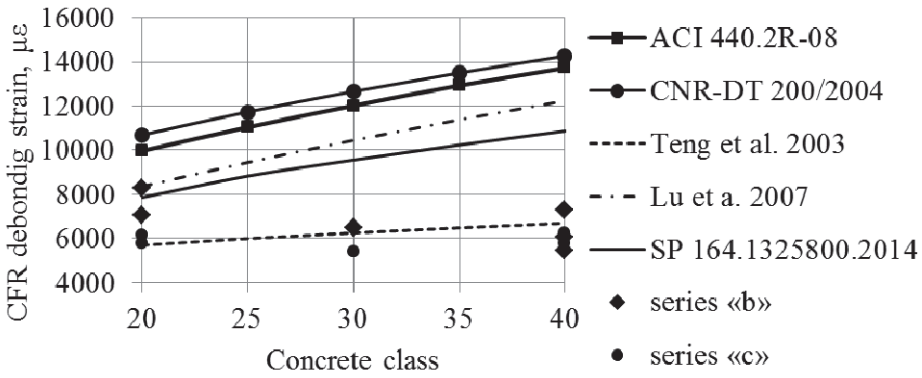

Figure 5: The comparison of experimental and theoretical values of deformations corresponding to the onset of cohesive delamination.

ACKNOWLEDGMENT

This research was supported by the Russian Science Foundation, project No. 14-29- 00172.

REFERENCES

[1] Teng, J.G., Failure modes of FRP-strengthened restructures, 26th Conference on Our World in Concrete & Structures: 27-28 August, Singapore (2001) 627-634.
[2] SP 164.1325800.2014. Strengthening of reinforced concrete structures with composite materials. design rules (2014) (in Russian).
[3] ACI 440.2R-08. Guide for the design and construction of externally bonded FRP systems for strengthening concrete structures. ACI (2008).
[4] Zhang, A., Jin, W., Li, G., Behavior of preloaded RC beams strengthened with CFRP laminates, Journal of Zhejiang University SCIENCE A, 7 (2006) 436-444.

[5] Parikh, K., Modhera, C.D., Application of GFRP on preloaded retrofitted beam for enhancement in flexural strength, International journal of civil and structural engineering, 2 (2012) 1070-1080.
[6] Al-Salloum, Y.A., Flexural behavior of rc beams strengthened with FRP composite sheets subjected to different load cases, King Saud University, Saudi Arabia. http://faculty.ksu.edu.sa/ysalloum/Documents/My%20Papers/Flexure%20UK%202006.pdf.
[7] Vavilov, V.P., Thermal/Infrared nondestructive testing, NDT Handbooks series, Moscow 5(2009).
[8] Concu, G., De Nicolo, B., Piga, C., Trulli, N., Infrared thermography as a tool for quality control of FRP and FRCM application, Proceedings of the 6th International conference on FRP composites in civil engineering. – Rome, (2012).
[9] Valluzzi, M.R., Grinzato, E., Pellegrino, C., Modena, C., IR thermography for interface analysis of FRP laminates externally bonded to RC beams, Materials and Structures, 42 (2009) 25-34.
[10] Shirazi, A., Karbhar, V.M., Quantifying defects and progression of damage in FRP rehabilitation of concrete through IR thermography, Asia-Pacific Conference on FRP in Structures (APFIS 2007). International Institute for FRP in Construction, (2007).
[11] Taillade, F., Quiertant, M., Benzarti, K., Dumoulin, J., Aubagnac, Ch., Nondestructive evaluation of FRP strengthening systems bonded on RC structures using pulsed stimulated infrared thermography, IFSTTAR, F-75015 Paris, (2012) 193-208.
[12] Bykov, A., Matveenko, V., Serovaev, G., Shardakov, I., Shestakov, A., Determination of thermography modes for recording delamination between composite material and reinforced concrete structures, Solid State Phenomena, TTP, (2016) 97-104.